



ELSEVIER

Journal of Chromatography B, 711 (1998) 3–17

JOURNAL OF  
CHROMATOGRAPHY B

## Driving forces for phase separation and partitioning in aqueous two-phase systems

Hans-Olof Johansson<sup>a</sup>, Gunnar Karlström<sup>c</sup>, Folke Tjerneld<sup>b</sup>, Charles A. Haynes<sup>a,\*</sup>

<sup>a</sup>*Biotechnology Laboratory, 237 Wesbrook Bldg, The University of British Columbia, Vancouver, British Columbia V6T 1Z3, Canada*

<sup>b</sup>*Department of Biochemistry, Chemical Center, University of Lund, P.O. Box 124, S-221 00 Lund, Sweden*

<sup>c</sup>*Department of Theoretical Chemistry, Chemical Center, University of Lund, P.O. Box 124, S-221 00 Lund, Sweden*

### Abstract

A set of simple analytical equations, derived from the Flory–Huggins theory, are used to identify the dominant driving forces for phase separation and solute (e.g., protein) partitioning, in the absence and presence of added electrolyte, in every general class of aqueous two-phase systems. The resulting model appears to capture the basic nature of two-phase systems and all trends observed experimentally. Case studies are used to identify fundamental differences in and the magnitudes of enthalpic and entropic contributions to partitioning in polymer–polymer (e.g., PEG–dextran), polymer–salt, and thermoseparating polymer–water (e.g., UCON–water) two-phase systems. The model therefore provides practitioners with a better understanding of partition systems, and industry with a simple, fundamental tool for selecting an appropriate two-phase system for a particular separation. © 1998 Elsevier Science B.V. All rights reserved.

*Keywords:* Aqueous two-phase systems; Partitioning; Flory–Huggins theory; Proteins

### 1. Introduction

Following the pioneering work of Albertsson [1], aqueous two-phase systems are finding increasing use in extractive separations and high-sensitivity assays of biomaterials [2]. Aqueous two-phase systems are formed by mixing one or more polymers or surfactants with water, and can, for instance, be used to selectively partition and purify target proteins from culture supernatant or lysate. Well-studied two-phase systems include poly(ethylene glycol) (PEG)–dextran and PEG–phosphate, where each phase generally contains 80% (w/w) to 95% water. This high water content, combined with the low interfacial tension of the system, allows for nondestructive

partitioning of sensitive biomaterials such as proteins, cell organelles, and whole viable cells [2].

New types of aqueous two-phase systems are now being developed in which a thermoseparating polymer serves as a phase-forming component. Binary aqueous solutions of a thermoseparating polymer split into two equilibrium phases above a critical temperature, referred to as the cloud point [3,4]. The most common class of water-soluble thermoseparating polymers are random copolymers of ethylene oxide (EO) and propylene oxide (PO), henceforth collectively called EOPO polymers. Thermoseparated water–EOPO two-phase systems are composed of an almost pure water top phase and a polymer-rich bottom phase (usually containing 40–60% EOPO) [5]. Compared with conventional PEG–dextran systems, water–EOPO systems exhibit relatively large differences in phase hydrophobicities and free vol-

\*Corresponding author.

umes, suggesting that relatively large changes in enthalpy and entropy, respectively, accompany both phase separation and partitioning behavior. The same general argument holds for PEG–salt two-phase systems (e.g., PEG–phosphate), where both the solvent concentration and hydrophilicity of the salt-rich phase are significantly higher than in the PEG-rich top phase.

Water–EOPO two-phase systems have been used to separate amino acid mixtures and mixtures of polypeptides [6,7]. Native proteins are often excluded from the polymer-rich phase since they are in general too hydrophilic to be solubilized in the concentrated hydrophobic polymer phase [8–10].

Partitioning of low-molecular-mass proteins and other charged biomolecules can be enhanced, in some cases dramatically, by the addition of certain electrolytes to a phase system. Albertsson [2] and others [11–14] have shown that the addition of a single strong electrolyte to an initially uncharged aqueous two-phase system (e.g., PEG–dextran or water–EOPO) will lead to the formation of a Galvani-type interfacial electrostatic potential difference  $\Delta\psi$  if the anion(s) and cation(s) of the dissociated salt have different affinities for the two phases. This interfacial potential difference will contribute to the overall partition coefficient of a protein macro-ion in direct proportion to the net charge  $z_p$  of the protein at the system pH, bearing in mind that a partitioned protein macro-ion must carry with it a sufficient number of counter-ions and co-ions to maintain phase electroneutrality.

The magnitude (typically in the  $\sim 30$  to  $30$  mV range) and sign of  $\Delta\psi$  are determined by the partitioning behavior of ions of the majority salt in the system. In PEG–salt two-phase systems, the phase-forming salt will therefore determine  $\Delta\psi$ . For example,  $\Delta\psi$ , defined as  $\psi^t - \psi^b$  where  $t$  is the top phase and  $b$  the bottom, is positive for the PEG–phosphate and PEG–sulfate systems so that it favors partitioning of net negatively charged proteins into the PEG-rich top phase. As a result, such systems are not well suited for selective partitioning and purification of proteins with high isoelectric points. The water–EOPO and PEG–dextran systems are more versatile in this respect. The occurrence of phase separation in the absence of added electrolyte allows one to manipulate the sign and magnitude of  $\Delta\psi$ , and

thus partitioning behavior, by selecting an appropriate salt (and salt concentration).

Other thermoseparating polymers which are currently being explored in aqueous two-phase partitioning applications include (1) triblock EOPO copolymers which form a micellar-rich phase above a critical micelle temperature (CMT) [15], and (2) uncharged surfactants which form a cylindrical-micelle-rich top phase above an LCST [16]. These and other new systems should expand the range of applications of aqueous two-phase technology to include, for instance, separation of membrane-bound proteins and the establishment of wider, more accurate hydrophobicity scales for proteins. However, the further expansion of our library of potentially useful aqueous two-phase systems exacerbates a problem that has plagued the technology from its inception. Namely, with hundreds of unique two-phase systems now having been discovered, how does one select the appropriate two-phase system for a given application? Here, we address this question by formulating a fundamental, yet simple model based on the Flory–Huggins mean-field theory for polymer solutions which describes the dependence of phase behavior and protein partitioning on system variables and configuration. Through a series of examples, we show that the model provides a relatively simple means of analysing and selecting appropriate aqueous two-phase systems for a particular separation or concentration process.

Many of the concepts used in the derivation of our model follow from the work of Brooks et al. [17], who was the first to show that Flory–Huggins theory provides a useful framework for describing phase separation and partitioning in two-phase systems. The simple, analytical equations which result from our model development are a departure from the more detailed fundamental statistical–mechanical models for partitioning systems, such as the integral-equation model of Haynes et al. [18] and the virial-expansion models of Kabiri-Badr and Cabezas [19], Döbert et al. [20] and others, as reviewed by Cabezas [21], which are more difficult to solve and are intended for quantitative prediction of system properties. In contrast, the simple mean-field model developed here is derived in a manner which allows for rapid qualitative interpretation of the dominant energetics, explicitly written in terms of enthalpic

and entropic contributions, driving phase separation and partitioning, as well as the dependence of these energetics on phase composition and structure. In particular, the model is intended for practitioners of aqueous two-phase technology who desire a set of simple, but fundamental model equations which allow them to understand the general nature of their systems and the general dependence of phase behavior and partitioning on system variables under direct experimental control.

## 2. Flory–Huggins theory applied to aqueous two-phase partition systems

By representing an unbranched polymer chain as a linear sequence of connected segments in which each segment occupies one site of a lattice composed of  $N$  total sites, Flory [22] and Huggins [23] derived an approximate expression for the entropy change  $\Delta S^c$ , known as the combinatorial entropy, accompanying mixing of pure amorphous polymer with pure solvent under conditions where there are no net attractive or repulsive interactions between components. Consider a lattice filled with  $m$  components so that the total number of lattice sites  $N$  is

$$N = \sum_{i=1}^m M_i n_i \quad (1)$$

where  $n_i$  is the number of molecules of component  $i$  and  $M_i$  is the degree of polymerization (i.e., the number of segments on the chain). The volume fraction  $\Phi_i$  of each component  $i$  in the system is then

$$\Phi_i = \frac{M_i n_i}{N} \quad (2)$$

For such systems, Flory derived the following expression for the combinatorial entropy  $\Delta S^c$

$$\Delta S^c = -NR \sum_{i=1}^m \frac{\Phi_i}{M_i} \ln \Phi_i \quad (3)$$

where  $R$  is the gas constant. To arrive at this simple expression, Flory assumed the system to be incompressible and thus neglected any contributions from pressure–volume work. Additional model assumptions are detailed elsewhere [22]; none of them affect the qualitative analysis presented here. Eq. (3)

predicts only positive values for  $\Delta S^c$ , indicating that in the absence of intermolecular interactions the components will mix to form a single homogeneous phase. However, Eq. (3) also predicts that the magnitude of  $\Delta S^c$  will decrease with increasing degree of polymerization  $M_i$  of each component  $i$ . Thus, although  $\Delta S^c$  favors mixing, its contribution to mixing is often significantly less than the ideal entropy change  $\Delta S^{\text{id}}$  accompanying mixing of small molecules of equal size (i.e.,  $0 < \Delta S^c < \Delta S^{\text{id}} = -NR \sum_{i=1}^m x_i \ln x_i$ , where  $x_i$  is the mole fraction of component  $i$ ). As a result, whereas demixing of small near-equal-sized components (e.g., benzene–water) requires fairly large solution nonidealities (i.e.,  $\Delta H^{\text{ex}} \gg 0$  and/or  $\Delta S^{\text{ex}} \ll 0$ , where superscript ex denotes excess property), small nonidealities can and often do lead to phase separation in dilute solutions of polymer(s) in a low-molecular-mass solvent.<sup>1</sup>

For example, a ternary aqueous mixture at 25°C of 20% (w/w) ethanol and 20% glucose, the monomeric units of PEG and dextran, respectively, is fully miscible. In contrast, as shown in Fig. 1, phase separation in an aqueous mixture of PEG 6000 and dextran T-500 occurs for polymer weight fractions as low as 5% and 0.5%, respectively (see Table 1 for details of the calculation). In both systems, the net nonideal interaction between the two nonaqueous components is slightly repulsive, but only in the polymeric system does this small repulsive energy overcompensate the favorable entropy of mixing.

Flory applied regular solution theory [26] to the lattice to introduce into his model an approximate expression for the mixing energy  $\Delta U_{\text{mix}}$  of a polymer solution

$$\Delta U_{\text{mix}} = N \sum_{i=1}^{m-1} \sum_{j=i+1}^m \Phi_i \Phi_j w_{ij} = \Delta H_{\text{mix}} \quad (4)$$

Since the lattice is assumed incompressible,  $\Delta U_{\text{mix}}$  is

<sup>1</sup>It should be noted that Flory's result (Eq. (3)) overpredicts by a factor of ~2 the decrease in mixing entropy which results from increasing the degree of polymerization of the polymer component(s). More accurate models for  $\Delta S^c$  have been derived [24,25]. The Flory result, however, captures the essential physics of the problem, which is all that is required for our qualitative analysis.

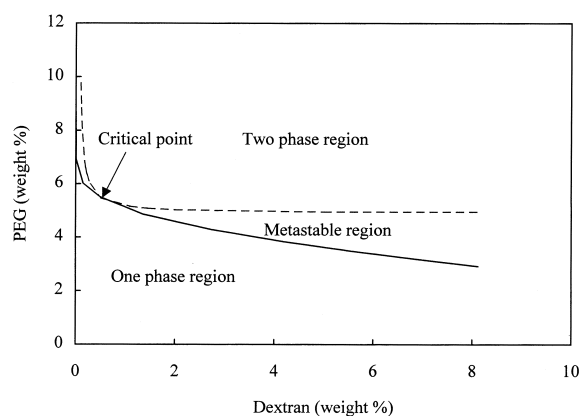


Fig. 1. Model calculated binodal (solid line) and spinodal (dashed line) curves for the PEG6000 and dextran T500 system. Degree of polymerization ( $M$ ) for water (1), PEG (2) and dextran (3) used in the calculations is:  $M_1=1$ ,  $M_2=100$  and  $M_3=10\,000$ . Interaction parameters (J/mol) are:  $w_{12}=100$ ,  $w_{13}=0$  and  $w_{23}=245$ . Temperature = 20°C.

equal to  $\Delta H_{\text{mix}}$ , the change in enthalpy when the pure components are mixed. The effective pair-wise interchange energy  $w_{ij}$  is defined as

$$w_{ij} = z(F_{ij} - \frac{1}{2}(F_{ii} + F_{jj})) \quad (5)$$

and is equal to one-half the energy required to exchange a molecule of type  $i$  in a solution of pure  $i$ , where the molecule interacts with  $z$  nearest neighbors, and a molecule of type  $j$  in a solution of pure  $j$

to form  $2z$  dissimilar ( $i-j$ ) pairs. In Eq. (5),  $F_{ii}$ , for instance, is the potential energy of an  $i-i$  pair. To explicitly account for thermal energy, the interchange energy is often replaced with the Flory interaction parameter  $\chi_{ij}$ , defined as  $w_{ij}/kT$ . The enthalpy change upon mixing may therefore be described by an appropriate set of  $w_{ij}$  or  $\chi_{ij}$  for all unlike binary interactions in the system. A positive value of either  $w_{ij}$  or  $\chi_{ij}$  indicates an endothermic (or enthalpically repulsive) net interaction between components  $i$  and  $j$ .

The Flory interaction parameter  $\chi_{ij}$  describing nonideal enthalpic binary interactions is a measurable quantity. It is a function of temperature but, in theory, not of composition. For the dilute aqueous polymer systems of interest here,  $\chi_{ij}$  values have been determined from low-angle laser-light scattering data [27] and differential-vapor-pressure data [28], and can also be determined from membrane-osmometry and vapor-pressure-osmometry experiments.

### 3. Phase stability and its dependence on system variables

Together, Eqs. (3) and (4) yield a qualitatively useful model for the Gibbs energy change  $\Delta G_{\text{mix}}$  accompanying mixing of polymers in solvent

Table 1

Interaction parameters and degrees of polymerization of the components for the calculated data in Table 1 and in Figs. 1,3–6

System	PEG–dextran	PEG–phosphate	EOPO–water
System composition (volume fraction)	6% PEG 8% dextran 0.01% solute	85.99% water, 10% PEG 3% Na <sup>+</sup> , 1% PO <sub>4</sub> <sup>3-</sup> 0.01% solute	79.99% water 20.00% EOPO polymer 0.01% solute
Interaction parameters (J/mol)	$w_{12}=100$ , $w_{13}=0$ , $w_{1s}=0$ , $w_{23}=245$ , $w_{2s}=-100$ , $w_{36}=0$	$w_{14}=-10\,000$ , $w_{15}=-30\,000$ , $w_{24}=-1000$ , $w_{25}=-3000$ , $w_{4s}=-1000$ , $w_{5s}=-3000$ $w_{45}=-50\,000$	$w_{1p}=546$ , $w_{1u}=6188$ , $w_{pu}=440$ , $w_{ps}=-100$ , $w_{us}=-100$ , $w_{uu}=5121$
Degree of polymerisation and temperature	$M_1=1$ , $M_2=100$ , $M_3=10\,000$ , $M_s=1$ $T=20^\circ\text{C}$	$M_4=1$ , $M_5=1$ $T=20^\circ\text{C}$	$M_{\text{polymer}}=217$ $T=70^\circ\text{C}$

All interaction parameters are effective.

Subscripts: 1=water, 2=PEG, 3=dextran, 4=Na<sup>+</sup>, 5=PO<sub>4</sub><sup>3-</sup>, s=solute, p=polar form of EOPO polymer, u=unpolar form of EOPO polymer, for calculation of phase diagram see [8].

$$\begin{aligned}\Delta G_{\text{mix}} &= \Delta H_{\text{mix}} - T\Delta S^c \\ &= NRT \sum_{i=1}^m \frac{\Phi_i}{M_i} \ln \Phi_i + N \sum_{i=1}^{m-1} \sum_{j=i+1}^m \Phi_i \Phi_j w_{ij}\end{aligned}\quad (6)$$

Provided the required set of measured (or calculated)  $\chi_{ij}$  are available at system temperature, Eq. (6) may be minimized as a function of composition to estimate the phase diagram and, under conditions where the mixture phase separates, the compositions of the equilibrium phases (i.e., the coexistence curve and associated equilibrium tie-lines) [5]. Eq. (6) therefore encodes much of the basic physics of phase behavior in polymer–polymer aqueous-two-phase systems. However, as with many of the more advanced models describing two-phase systems [18], it is difficult to establish a basic understanding of phase behavior (and its dependence on system variables such as polymer molecular mass) through inspection of Eq. (6).

Stability analysis offers a more direct approach for determining the influence of system variables on phase behavior. Let us consider, for instance, a ternary mixture containing water (1) and polymers 2 and 3. The condition for incipient instability is specified by the spinodal curve. For a ternary mixture at constant temperature and pressure, Tompa [29] has shown that the spinodal curve for a ternary incompressible system is defined by

$$\left(\frac{\partial^2 \Delta G_{\text{mix}}}{\partial \phi_2^2}\right)_{T,V,\phi_3} \left(\frac{\partial^2 \Delta G_{\text{mix}}}{\partial \phi_3^2}\right)_{T,V,\phi_2} - \left(\frac{\partial^2 \Delta G_{\text{mix}}}{\partial \phi_2 \partial \phi_3}\right)_{T,V}^2 = 0 \quad (7)$$

Insertion of Eq. (6) into Eq. (7) yields the following simple result:

$$\sum_{i=1}^3 \frac{M_i \phi_i}{(1 - 2\chi_i M_i \phi_i)} = 0 \quad (8)$$

where  $2\chi_i = \chi_{ij} + \chi_{ik} - \chi_{jk} = (w_{ij} + w_{ik} - w_{jk})/kT$  ( $i \neq j \neq k$ ). As illustrated in Fig. 1, a one-phase mixture of total composition within the region inside the spinodal is unstable, and that between the spinodal and coexistence curve is metastable (where a one-phase solution can exist in the absence of active nucleation sites).

The resulting analytical equation for the spinodal predicts, among many things, that incipient instabili-

ty will not be reached if all  $\chi_i = 0$  since each term in Eq. (8) will then be greater than zero. In polymer–polymer aqueous two-phase systems such as the PEG–dextran system,  $\chi_{12}$ ,  $\chi_{13}$  and  $\chi_{23}$  are usually all positive in value and lie between  $\sim 0.1$  and  $0.8$  [30]. For such systems, Eq. (8) can be satisfied if  $\chi_{23} > \chi_{12} + \chi_{13}$ , indicating that the repulsive interactions between unlike polymer segments are stronger than the two polymer–solvent interactions.

To more simply illustrate the occurrence of phase instability when  $\chi_{23} > \chi_{12} + \chi_{13}$ , we can consider a particular case in which  $\chi_{12} \approx \chi_{13}$  (i.e., the two polymers interact with the solvent with similar energetics) and both  $\chi_{12}$  and  $\chi_{13}$  are small compared to  $\chi_{23}$ . Eq. (8) can then be simplified to yield the following result when  $\phi_1$  is close to unity, which is true near the critical point for most polymer–polymer aqueous two-phase systems

$$-2w_{23} + RT \left( \frac{1}{\phi_2 M_2} + \frac{1}{\phi_3 M_3} \right) = 0 \quad (9)$$

Whereas Eq. (8) is exact, we emphasize that Eq. (9) is approximate. Nevertheless, it qualitatively predicts much of the phase behavior of the traditional polymer–polymer aqueous two-phase systems used for partitioning (e.g., the PEG–dextran system). The first and second terms on the left-hand-side of Eq. (9) are the dominant enthalpic and entropic contributions to incipient instability, respectively, under these conditions. As noted above, the combinatorial entropy change upon mixing (Eq. (3)) is always positive, and therefore cannot on its own lead to phase instability. Near the critical point, Eq. (9) predicts that the amount to which entropy favors homogeneous mixing is directly proportional to temperature, and inversely proportional to the molecular masses and the volume fractions of the two polymers. Thus, the stability of the one-phase region will increase with increasing temperature, and decrease with increasing size or concentration of either polymer. Qualitatively, this is what is observed in aqueous two-phase systems. For example, measured critical points for ternary aqueous mixtures of PEG and dextran T-500 (also called dextran D-48) at  $20^\circ\text{C}$  decrease with increasing molecular mass of PEG in accordance with Eq. (9) [2].

Before proceeding, we note that Eq. (8) can be satisfied in a number of ways. For example, instabili-

ty can be reached when the two solvent–polymer interaction parameters ( $\chi_{12}$  and  $\chi_{13}$ ) are significantly different and near 0.5, and  $\chi_{23} \leq 0$ . In this case, the two-phase envelope becomes a closed loop, rather than the semi-hyperbolic shape observed in measured coexistence curves for aqueous two-phase systems [31]. Phase instability is also predicted when all  $\chi_{ij}$  are attractive. Depending on the magnitude of  $\chi_{23}$  relative to  $\chi_{12} + \chi_{13}$ , this can either lead to the formation of a polymer–polymer two-phase system (segregative phase separation) or a near pure-water phase and a concentrated phase enriched with both polymers (associative phase separation).

#### 4. Dependence of partitioning on system variables

When formulated properly, Flory–Huggins theory yields a simple analytical expression for the partition coefficient  $K_s$  of an infinitely dilute uncharged solute  $s$  which accounts for the dependence of phase-system variables such as degree of polymerization of the phase-forming components, temperature, and solute molecular mass. In this qualitative model, the enthalpic and entropic contributions to  $K$  are explicit, thereby allowing straightforward interpretation of the dominant energetics driving partitioning in a given two-phase system. To illustrate, we analyze the partitioning behavior of a model protein  $s$  in the three most common classes of aqueous two-phase systems: (1) PEG–dextran systems (representative of all polymer–polymer two-phase systems), (2) PEG–salt systems and (3) thermoseparated water–EOPO systems. We also use the model to evaluate the effect of polydispersity on phase behavior and partitioning.

$K_s$  is defined as the volume fraction of solute  $s$  in the top phase  $\phi_s^t$  divided by  $\phi_s^b$ , the volume fraction of  $s$  in the bottom phase. Its determination therefore requires knowledge of the compositions of the two equilibrium phases. In general, this requires numerical solution of a set of  $m$  nonlinear equations (where  $m$  is the number of system components) generated from the phase-equilibria criteria

$$\mu_i^t = \mu_i^b \quad (10)$$

where  $\mu_i^t$  is the chemical potential of component  $i$  in the top phase and is given by

$$\begin{aligned} \mu_i^t &= \left( \frac{\partial \Delta G_{\text{mix}}^t}{\partial n_i^t} \right)_{T,P, \text{ all } n_j \neq n_i} \\ &= \mu_i^o + RT \ln \phi_i^t + (\mu_i^{\text{ex}})^t \end{aligned} \quad (11)$$

In Eq. (11),  $\mu_i^o$  is the chemical potential of pure component  $i$  at system temperature, and  $\mu_i^{\text{ex}}$  is the excess chemical potential of  $i$  in the phase. If, however, the solute is infinitely dilute, we can assume that its addition will not alter the compositions of the equilibrium phases. This greatly simplifies the analysis. The infinite-dilution assumption has therefore been used by a number of theoreticians [17,32,33] to derive approximate analytical expressions for the partition coefficient. Under such conditions,  $K_s$  can be determined directly from the solute-free phase diagram and application of Eqs. (10) and (11) to solute  $s$

$$\ln K_s = \ln \left( \frac{\phi_s^t}{\phi_s^b} \right) = \frac{1}{RT} [(\mu_s^{\text{ex}})^b - (\mu_s^{\text{ex}})^t] \quad (12)$$

Here,  $(\mu_s^{\text{ex}})^b$ , for instance, accounts for the excess entropy of mixing the phase-forming components, and the nonideal interactions between all unlike pairs present in the bottom phase (e.g., protein–polymer, polymer–solvent, etc.).

##### 4.1. Entropic contribution to the partition coefficient

Application of Eq. (11) to Eq. (6) assuming  $\Delta H_{\text{mix}}$  is equal to zero yields the entropic contribution to the chemical potential of solute  $s$

$$\begin{aligned} \mu_s - \mu_s^o &= -T \left( \frac{\partial \Delta S^c}{\partial n_s} \right)_{T,P, n_j \neq n_s} \\ &= RT \left[ \ln \phi_s - \phi_s + 1 - M_p \sum_{i \neq s}^m \frac{\phi_i}{M_i} \right] \end{aligned} \quad (13)$$

The logarithmic term in the brackets ( $RT \ln \phi_s$ ) gives the ideal change in partial molar entropy accompanying mixing of solute  $s$  with the phase. The remaining three terms represent  $\mu_s^{\text{ex}}$  as defined in Eq. (11). The solute partition coefficient is therefore given by

$$\begin{aligned} \ln K_s &= -(\phi_s^t - \phi_s^b) + M_s \left( \sum_{i \neq s}^m \frac{\phi_i^t}{M_i} - \sum_{i \neq s}^m \frac{\phi_i^b}{M_i} \right) \\ &= M_s \left( \sum_{i \neq s}^m \frac{\phi_i^t}{M_i} - \sum_{i \neq s}^m \frac{\phi_i^b}{M_i} \right) \end{aligned} \quad (14)$$

where the second equality follows from the fact that at infinite dilution, both  $\phi_s^t$  and  $\phi_s^b$  are vanishingly small and, thus,  $\phi_s^t - \phi_s^b = 0$ .

A clear physical interpretation of Eq. (14), and thus the entropic contribution to partitioning, can be gained by noting that  $(\phi_i^t/M_i) = (n_i^t/N^t) = (n_i^t/\rho V^t)$ , where  $N^t$  is the total number of lattice sites in the top phase;  $\rho$  is the number of lattice sites per unit volume, and  $V^t$  is the volume of the top phase. Eq. (14) then reduces to

$$\ln K_s = \frac{M_s}{\rho} \left( \frac{n^t}{V^t} - \frac{n^b}{V^b} \right) \quad (15)$$

where  $n^t$  and  $n^b$  are the total number of molecules in the top and bottom phase, respectively. This simple relation indicates that in the absence of enthalpic effects, uneven partitioning will result if there is a difference between the top and bottom phases in the number of molecules per unit volume (i.e., the number density). Under such conditions, the solute will partition to the phase with the highest number density. This follows from the fact that the mixing entropy increases in proportion to the natural logarithm of the number of distinguishable ways in which the molecules in the mixture can be arranged. In essence, the phase with the higher number density can accommodate the solute in more ways, thereby increasing its partitioning to that phase.

It is interesting to evaluate the influence of this entropic effect on partitioning in the three general types of two-phase systems described above. In a typical PEG–dextran two-phase system, the number density of the PEG phase is somewhat higher than the dextran phase due to the higher water content of the top phase. Eq. (15) predicts that solute  $s$  will partition to the top phase. The effect, however, is small since the two phases contain similar and significant amounts of water, which makes the dominant contribution to the number density of the phase.

Entropic effects on partitioning are significantly larger for PEG–salt systems and, in particular,

thermoseparated two-phase systems such as water–EOPO. In both systems, the polymer component is effectively localized in one phase, causing the number density of the phase to be considerably lower than the opposing water-rich phase. As shown in Eq. (15), there is a strong entropic driving force for solute partitioning into the polymer-free phase of such systems which increases linearly with the size ( $M_s$ ) of the solute.

An example of the entropic effect described by Eq. (15) is provided by Liu et al. [16], who studied the partitioning of several globular proteins and bacteriophage T4 in thermoseparated aqueous micellar systems. Nonionic alkyl poly(ethylene oxide)-type surfactants phase separate in water into a cylindrical micelle-rich phase, which has a very low number density, and a near pure-water bottom phase. Proteins introduced into this system partition strongly to the water-rich phase in accordance with their molecular masses. Because of their colloidal size (i.e., very large  $M_s$ ), bacteriophages partition almost exclusively ( $\sim 1000$  to 1) to the water-rich phase. Although some of this dramatic partitioning effect may be enthalpically driven due to the hydrophilic surface properties of proteins, it provides strong qualitative evidence of the importance of entropic effects in systems with phases which differ significantly in number density.

#### 4.2. Enthalpic contribution to the partition coefficient

Consider now a system where excess entropy contributions to partitioning are negligible: for instance, a two-phase system where the number densities of the phases are identical. The partitioning of a protein will then only depend on the difference in the partial molar enthalpy of the protein  $\bar{h}_s$  in the top and bottom phases. At infinite dilution, the partial molar enthalpy of protein  $s$  is given by

$$\begin{aligned} \bar{h}_s &= \left( \frac{\partial \Delta H_{\text{mix}}}{\partial n_s} \right)_{T,P,n_j \neq n_s} \\ &= -M_s \sum_{i=1(i \neq s)}^{m-1} \sum_{j=i+1(j \neq s)}^m \phi_i \phi_j w_{ij} \\ &\quad + M_s \sum_{i=1(i \neq s)}^m \phi_i (1 - \phi_s) w_{is} \end{aligned} \quad (16)$$

Since the protein is infinitely dilute,  $\phi_s = 0$  and the last term simplifies to  $M_s \sum_{i=1(i \neq s)}^m \phi_i w_{is}$ .

In the absence of entropic nonidealities,  $\mu_s^{\text{ex}}$  is equal to  $\bar{h}_s$ . Eq. (12) then yields the following expression for the partition coefficient

$$\ln K_s = -\frac{M_s}{RT} \left[ \sum_{i=1(i \neq s)}^m (\phi_i^t - \phi_i^b) w_{is} - \sum_{i=1(i \neq s)}^{m-1} \sum_{j=i+1(j \neq s)}^m (\phi_i^t \phi_j^t - \phi_i^b \phi_j^b) w_{ij} \right] \quad (17)$$

The enthalpic contribution to solute partitioning contains two terms. The first is a summation which quantifies the energy difference due to all binary unlike enthalpic interactions between the protein and the remaining components in each phase (i.e., terms containing  $w_{is}$ ). The summation  $\sum_{i=1(i \neq s)}^m \phi_i^t w_{is}$  therefore represents the energy of interaction between a lattice site belonging to a protein and an average lattice site of the top (t) phase which, for simplicity, can be abbreviated as  $w_{ts}$ . The basic concept of this term is accounted for in virtually all models and correlations for partitioning in aqueous two-phase systems (e.g., [33]). In a PEG–dextran two-phase system, for instance, it states that a protein which has a significantly higher affinity for PEG than for dextran will partition into the PEG-rich phase.

The second term on the right-hand side of Eq. (17) is less intuitive but, as we will soon see, usually important and often dominant. It is a summation which quantifies the difference in energy of each phase due to unlike enthalpic interactions between all phase components other than the protein (i.e., terms containing  $w_{ij}$ , where  $i \neq j \neq s$ ). The double summation  $\sum_{i=1(i \neq s)}^{m-1} \sum_{j=i+1(j \neq s)}^m \phi_i^t \phi_j^t w_{ij}$  therefore gives the total enthalpy of formation of the top phase (in the absence of protein) divided by the number of lattice sites in the top phase. This ‘self energy’ of the top phase can be abbreviated as  $E_t$ . Eq. (17) then simplifies to

$$\ln K_s = -\frac{M_s}{RT} [(w_{ts} - E_t) - (w_{bs} - E_b)] \quad (18)$$

where subscript b represents the bottom phase. Both  $w$  and  $E$  in Eq. (18) are energies. Negative values therefore represent an energetically favorable process and positive values an unfavorable process. For

example, if the protein has a strong attraction for a component which is enriched in the top phase, then  $w_{ts}$  will be more negative (or less positive), which leads to a more positive (or less negative) value of  $\ln K_s$ .

The dependence of  $K_s$  on the self energies of the top and bottom phases arises because insertion (partitioning) of a protein solute into a phase requires breaking interactions between components of the phase to create a cavity into which the protein fits. If those interactions are attractive, then disrupting them is energetically unfavorable. If however the interactions are repulsive, then formation of the cavity is favorable. In essence, the self energy of a phase is the energy of interaction between two average lattice sites of the phase. Eq. (18) predicts that the protein will favor partitioning to the phase with the highest (more positive) self energy  $E$ .

The self energy of a phase becomes more positive with increasing concentration of components which have a repulsive interaction for each other. For example, in a PEG–phosphate two-phase system, the PEG phase has the higher self energy because it contains significant concentrations of PEG and sodium phosphate, which strongly repel. Similarly, the EOPO-rich phase in a thermoseparated water–EOPO system has the higher self energy because it is enriched with a nonpolar conformation of the polymer and contains appreciable amounts of water.

As shown in Eq. (15), the entropic contribution to partitioning has no direct dependence on temperature. Eq. (18) indicates that enthalpically, partitioning will become less extreme with increasing temperature. Both predictions, however, are valid only if the phase compositions and polymer conformations do not change significantly with temperature.

#### 4.3. Relative magnitudes of enthalpic and entropic contributions to partitioning: some case studies

Within the infinite-dilution approximation, the solute partition coefficient is given by the sum of Eqs. (15) and (18)

$$\ln K_s = -\frac{M_s}{RT} [(w_{ts} - E_t) - (w_{bs} - E_b)] + \frac{M_s}{\rho} \left( \frac{n^t}{V^t} - \frac{n^b}{V^b} \right) \quad (19)$$



In Eq. (19),  $\ln K_s$  varies linearly with the degree of polymerization  $M_s$  in both the enthalpic and entropic contributions. Flory–Huggins theory therefore predicts that a polymerized or multimeric form of a solute will prefer the same phase as the monomeric form, but to a proportionally greater extent. An important example of this is the well-known effect of dextran polydispersity on the PEG–dextran phase diagram. Several groups have observed that when a polydisperse fraction of dextran is used to establish a two-phase system, the higher-molecular-mass chains are enriched in the dextran-rich phase, while the PEG-rich phase contains a slight excess of low-molecular-mass dextran (e.g., [34]). In PEG–dextran two-phase systems, the number density of the PEG-rich phase is larger. Entropically, then, the higher-molecular-mass dextran chains should partition more strongly to the PEG-rich phase, opposite to what is observed. Enthalpy effects must therefore lead to enrichment of the dextran-rich phase with high-molecular-mass chains.

In PEG–dextran systems, the PEG-rich phase has the higher self energy due to the unfavorable interaction between PEG and water. This indicates that the self energy term, like the entropic contribution, favors enrichment of the PEG-rich phase with high-molecular-mass dextran chains. The direct-interaction ( $w_{ts} - w_{bs}$ ) contribution to  $\ln K_s$  must therefore be sufficiently favorable to overcompensate the entropic and self-partitioning terms. Measured osmotic second virial coefficients for the PEG–dextran system agree with this observation [18,30]. The Flory interaction parameter  $\chi_{23}$  regressed from osmotic second virial coefficient data is sufficiently positive to make the direct-interaction term the dominant contribution [28].

This effect of solute size on partitioning is seen more clearly in Fig. 2, which shows partition coefficients for several homopeptides in a thermoseparated water–EOPO system measured by Johansson et al. [7]. The hydrophilic amino acid glycine and the hydrophobic amino acid tryptophan favor partitioning to the water-rich and polymer-rich phases, respectively, in proportion to the length of the homopeptide.

Table 2 presents a comparison of the relative magnitudes of the entropic, direct-interaction (enthalpic) and self energy (enthalpic) terms in Eq. (19), and their contribution to solute partitioning in typical

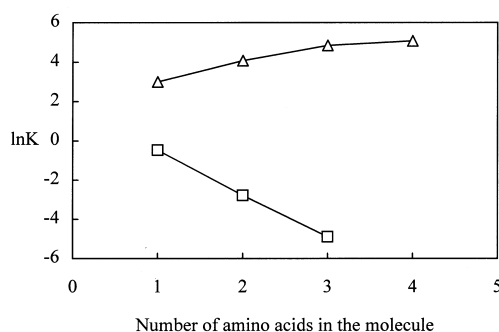


Fig. 2. Partitioning of amino acids and homopeptides in thermoseparated EOPO–water two-phase systems. The top phase contains ~100% water and the bottom phase ~60% EOPO and ~40% water. Temperature: 60°C. ( $\Delta$ ) Glycine or glycyl peptide and ( $\square$ ) tryptophan or tryptophanyl peptides. Data from [7].

PEG–dextran, PEG–phosphate, and water–EOPO two-phase systems. All parameters and other information required for the calculations are provided in Table 1. In each case, the values reported are normalized against the  $M_s$  of an infinitely-dilute uncharged solute which has a small attractive interaction with PEG or the EOPO polymer.

In the PEG–dextran system, the entropic contribution is small, always favoring partitioning to the PEG-rich phase which has a slightly larger number density assuming, as is usually the case, that PEG is the lower-molecular-mass polymer. The self-energy term is also small and always favoring partitioning to the PEG-rich phase. Depending on the nature of the solute, the direct-interaction term can provide a small driving force for partitioning to either phase. As a result,  $(\ln K_s)/M_s$  is typically near zero in PEG–dextran systems, indicating that extreme partitioning will only be observed for large solutes (i.e., large  $M_s$ ).

In contrast, partitioning in the PEG–phosphate and water–EOPO systems is the result of large contributions from the entropic and self-energy terms. In both cases, the polymer-free phase has a significantly higher number density, while the polymer-rich phase (the top phase in the PEG–phosphate systems, and the bottom phase in the water–EOPO system) has the higher self energy. In the PEG–phosphate system, a large difference in self energies is created by the strong attraction of the salt to water. This enthalpic effect sufficiently compensates the high

Table 2

Model calculations of the partitioning of a small cosolute (degree of polymerization=1) in three different systems

Phase systems top/bottom	PEG–dextran	PEG–phosphate	Water–EOPO
$\ln K_s$	0.0111	0.056	0.3282
$(w_{ts} - w_{bs})/RT$	-0.0048	0.0155	0.0199
$(E_t - E_b)/RT$	0.0038	0.2476	-0.2148
$(n_t/V_t - n_b/V_b)/\rho$	0.0025	-0.1761	0.5629

Phase composition and interaction parameters are listed in Table 1.

$n_t/(\rho V_t)$  is the number density in the top phase=number of molecules/volume unit.  $w_{ts}$  is the average interaction between the solute and the top phase (subscript s and t, respectively).  $E_t$  is the top phase self energy, i.e. the average interaction between two lattice sites in the top-phase.  $w_{bs}$ ,  $E_b$ ,  $n_b/(\rho V_b)$  are the corresponding terms for the bottom phase.

number density of the salt-rich phase to make the direct-interaction term significant.

Entropic effects tend to dominate partitioning in thermoseparated water–EOPO systems due to the high concentration of polymer in the bottom phase and the near pure-water top phase. Thus, although the high self-energy of the polymer-rich phase will partially compensate this effect, selective partitioning to the polymer-rich phase requires a strong attraction of the solute for thermoseparated EOPO. The water–EOPO system is therefore only suitable for partitioning of hydrophobic molecules (such as denatured proteins or tryptophan-rich peptides), or for solution concentration by selective water removal (similar arguments hold for the micellar two-phase systems of Liu et al. [16]).

#### 4.4. Effect of polymer molecular mass on partitioning

The strong influence of polymer molecular mass on protein partitioning has been shown experimentally by several groups [35,36]. In one of the first analyses of aqueous two-phase systems using Flory–Huggins theory, Albertsson et al. [35] identified PEG–dextran two-phase systems, differing only in dextran molecular mass, which exhibit identical (or nearly identical) phase compositions. By partitioning several globular proteins in these systems, they showed that the partition coefficient increases with increasing molecular mass of the dextran, a result predicted by Flory–Huggins theory. Their experimental results for a small (ovalbumin) and a large (phosphofructokinase) globular protein are

shown in Fig. 3. For both proteins, the change in partitioning is larger when the molecular mass of dextran is low. The effect, however, is significantly greater for the high-molecular-mass protein.

As shown by Albertsson et al. [35], application of Flory–Huggins theory to the prediction of the change in  $\ln K_s$  with increasing polymer molecular mass (holding phase compositions constant) yields the following simple result

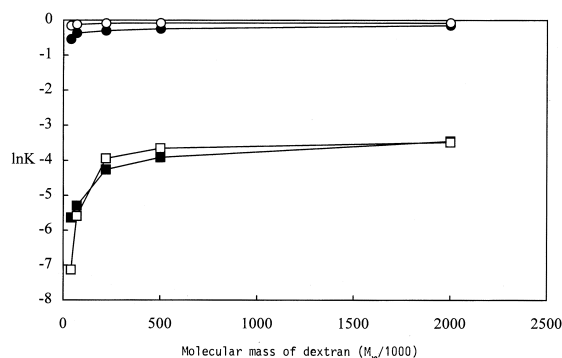


Fig. 3. Partitioning of proteins in PEG–dextran systems with different molecular masses of dextran. Polymer composition: 6% PEG and 8% dextran. Molecular mass of PEG is 6000. Filled symbols are data for hypothetical proteins (subscript s, solute) with same interaction parameters (J/mol),  $w_{ts}=0$ ,  $w_{2s}=150$  and  $w_{3s}=0$ . Polymer–polymer and polymer–water interaction parameters as Fig. 1. Degree of polymerization ( $M$ ) of calculated proteins are: (○);  $M=100$  and (□);  $M=4500$ . Experimental data for phosphofructokinase (■) and ovalbumin (●) are taken from [35]. Calculated degrees of polymerization of the dextrans are 1333, 2167, 6500, 10 000 and 15 556. The values are proportional to the number average molecular mass ( $M_n$ ). The degree of polymerization of dextran T500 is set to 10 000. Its  $M_n$  is  $180 \times 10^3$  [35]. Temperature = 20°C.

$$\begin{aligned} \Delta \ln K_s &= \ln K_s(1) - \ln K_s(2) \\ &= M_s c \left( \frac{1}{M_{\text{dextran}(1)}} - \frac{1}{M_{\text{dextran}(2)}} \right) \end{aligned} \quad (20)$$

where  $c$  is a constant given by the concentration of dextran in the top phase minus that in the bottom phase. Thus,  $c$  is a negative number. As indicated by Eq. (19), all enthalpic contributions to partitioning cancel under such conditions. The observed effect of increasing the dextran molecular mass  $M_{\text{dextran}}$  is therefore purely entropic, due to the resulting decrease in the number density of the bottom phase. In accordance with experiment, Eq. (20) predicts that increasing  $M_{\text{dextran}}$  will lead to an increase in  $\ln K_s$  (see Fig. 3) and thereby improve solute partitioning to the PEG-rich phase. Eq. (20) also predicts that the effect will increase linearly with solute molecular mass. Thus, the partitioning of large proteins is more sensitive to changes in polymer molecular mass, which is also observed.

#### 4.5. Effect of tie-line length on partitioning

Albertsson [2] has shown that partitioning also becomes more extreme with increasing tie-line length. For instance, Fig. 4 shows measured partition coefficients in a typical PEG–dextran two-phase system for serum albumin, which partitions preferentially to the bottom phase, and for phycoerythrin, which partitions to the top phase. As is often observed,  $\ln K_s$  for both proteins shows a slight nonlinear dependence on tie-line length. In accordance with Eq. (19), this suggests that  $\ln K_s$  is determined by a number of compensating effects, at least one of which has a nonlinear dependence on tie-line length. To better understand this, we have used Eq. (19) to calculate a series of partitioning curves (see Fig. 4) which differ only in the value of the solute–PEG interaction parameter,  $w_{2s}$ . All remaining  $w_{is}$  parameters are set equal to zero. Thus, the direct interaction terms in Eq. (19) are net attractive in the top phase when  $w_{2s} < 0$ , and repulsive when  $w_{2s} > 0$ . As shown in Fig. 4, the model does an excellent job of capturing the nonlinear behavior of  $\ln K_s$  for bovine serum albumin.

Fig. 4 also shows that partitioning to the bottom dextran-rich phase will only occur if  $w_{2s}$  is large and

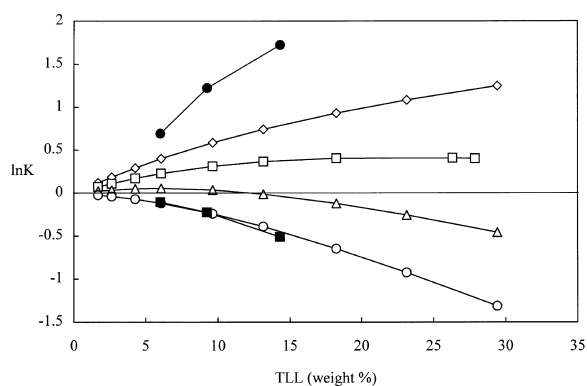


Fig. 4. Effect of TLL on the partitioning of proteins in PEG6000–dextran T500 systems.  $TLL = (\Delta C_{\text{PEG}}^2 + \Delta C_{\text{dextran}}^2)^{0.5}$ , where  $\Delta C_{\text{PEG}}$  and  $\Delta C_{\text{dextran}}$  are the differences in concentrations between the phases, for PEG and dextran, respectively. Unfilled symbols are data for hypothetical, calculated proteins (subscript  $s$ , solute). PEG–protein interaction parameters  $w_{2s}$  (J/mol) are: ( $\diamond$ );  $-50$ , ( $\square$ );  $50$ , ( $\triangle$ );  $150$  and ( $\circ$ );  $250$ . All protein dextran interactions = 0. Degree of polymerization for all calculated proteins is 100. All calculated polymer–polymer and water–polymer interactions and component sizes as in Fig. 1. Experimental data for serum albumin ( $\blacksquare$ ) and phycoerythrin ( $\bullet$ ) are taken from [2]. Temperature = 20°C.

positive, indicating a strong net repulsion for PEG. In PEG–dextran systems, both the entropic and the self-energy contributions to  $\ln K_s$  always favor solute partitioning to the top phase. Thus, the direct-interaction term must be sufficiently large to compensate both of these effects.

For the model result in Fig. 4 where  $w_{2s} = 150$  J mol $^{-1}$ , Fig. 5 shows the contributions of the entropic, self energy and direct-interaction terms to  $\ln K_s$  as a function of tie-line length. Partitioning in PEG–dextran system is usually carried out at tie-line lengths between 10 and 30 (wt% polymer). Over this range, the two enthalpic contributions show a linear dependence on tie-line length. (We note that at polymer concentrations far greater than used in experimental two-phase systems, the self-energy term becomes nonlinear and ultimately returns to zero at the solvent free limit.) The nonlinear dependence of  $\ln K_s$  on tie-line length shown in Fig. 4 is therefore based on entropic effects. Fig. 5 shows that the difference in number densities of the phases has a strong dependence on phase compositions near the critical point.

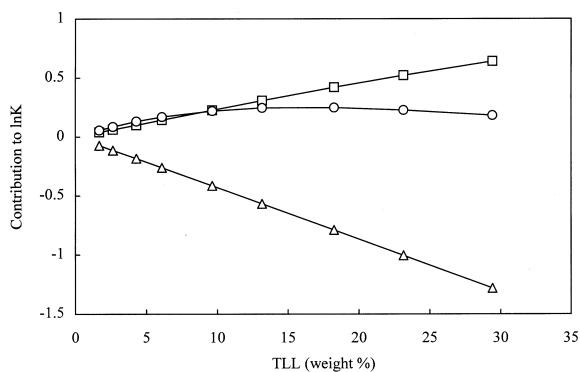


Fig. 5. Contributions to  $\ln K$  in terms of average interaction ( $w$ ), phase self energy ( $E$ ) and phase number density ( $n/V$ ) for increasing TLL. The phase systems are the same as in Fig. 4. The contributions are given as differences between the phases,  $(-\Delta w/RT)$  ( $\Delta$ ),  $\Delta E/RT$  ( $\square$ ) and  $\Delta(n/V)$  ( $\circ$ ), top – bottom, respectively. The  $\Delta E/RT$  and  $\Delta(n/V)$ , are the same for all proteins in Fig. 4. The  $-\Delta w/RT$  is given for the protein with  $w_{2s} = 150$  J/mol. All calculated polymer–polymer and water–polymer interactions and component sizes as in Fig. 1. Temperature = 20°C.

## 5. Simple interpretation of the effects of added electrolyte

At equilibrium, each phase of an aqueous two-phase system must be electrically neutral. This simple condition places clear and strict conditions on the way in which charged species, including protein macro-ions, can distribute between the two phases. For example, the movement of any ion from one phase to the other must involve the transfer (or counter-transfer) of a sufficient number of counterions (or co-ions) to maintain electroneutrality in both phases. As a result, the condition of phase electroneutrality, when combined with the laws of chemical and phase equilibrium, provides an unambiguous method for analyzing the strong and often curious dependence of protein partitioning on added electrolyte. To illustrate, we examine the effect of a single added electrolyte, containing only one type of cation of charge  $z_+$  and one type of anion of charge  $z_-$ , on the partition coefficient of a protein at infinite dilution. Our derivation follows from the now classic development of Albertsson [2] which has been used by several others to analyze charge effects [13,14].

For a two-phase system containing a single electrolyte (salt), phase electroneutrality requires that

$$\ln K_{\text{salt}} = \ln K_{\text{C}} = \ln K_{\text{A}} \quad (21)$$

where subscripts C and A denote the cation and anion, respectively, of the salt  $C_{\nu_+}A_{\nu_-}$ . Following Guggenheim [37], Albertsson [2] has shown that the partition coefficient of either ion  $i$  is given by

$$\ln K_i = \ln K_i^o + \frac{z_i F}{RT} \Delta\psi \quad (22)$$

where  $F$  is Faraday's constant,  $\Delta\psi$  is the interfacial electrostatic potential difference, and  $K_i^o$  is the self partition coefficient of the ion.  $K_i^o$  represents all contributions to the partition coefficient of ion  $i$  (and the activity coefficient of  $i$ ) other than the electrostatic work of moving the ion against the electrostatic potential gradient  $\Delta\psi$ . In principle,  $K_i^o$  can be determined from the distribution of an uncharged test molecule which has the same size, shape and molecular mass as ion  $i$ , and which interacts with the components of each phase in the exact same manner as ion  $i$ .

From Eqs. (21) and (22), the partition coefficient of the salt can be written in terms of the self partition coefficients of the cation and anion

$$\begin{aligned} \ln K_{\text{salt}} &= \frac{\nu_+}{\nu_+ + \nu_-} \ln K_{\text{C}} + \frac{\nu_-}{\nu_+ + \nu_-} \ln K_{\text{A}} \\ &= \frac{\nu_+}{\nu_+ + \nu_-} \ln K_{\text{C}}^o + \frac{\nu_-}{\nu_+ + \nu_-} \ln K_{\text{A}}^o \end{aligned} \quad (23)$$

From the second equality in Eq. (23), we observe that although ion partitioning depends on  $\Delta\psi$ , the partition coefficient of the neutral salt does not. As a result, no information about the magnitude of  $\Delta\psi$ , or even its existence, is required to determine the partition coefficient of the salt [10,14,18].

Determination of the partition coefficient  $K_s$  of the infinitely dilute protein macro-ion also does not require knowledge of  $\Delta\psi$ . To prove this, we apply Eq. (22) to the protein  $s$  (and each ion of the electrolyte) and solve for  $\Delta\psi$

$$\begin{aligned} \frac{F\Delta\psi}{RT} = \text{Constant} &= \frac{\ln K_s - \ln K_s^o}{z_s} = \frac{\ln K_{\text{C}} - \ln K_{\text{C}}^o}{z_+} \\ &= \frac{\ln K_{\text{A}} - \ln K_{\text{A}}^o}{z_-} \end{aligned} \quad (24)$$

Combining this with Eq. (21) yields our central result

$$\ln K_s = \ln K_s^o + \frac{z_s}{z_+ - z_-} (\ln K_A^o - \ln K_C^o) \quad (25)$$

which states that the partition coefficient of the protein  $K_s$  can be determined solely from knowledge of  $K_i^o$  for each charged component. A quantitative value of  $\Delta\psi$  is therefore not required to describe or calculate phase equilibria. This point is essential, as direct determination of  $\Delta\psi$  appears impossible [14,38]. Eq. (25) also states that, in a system which contains only one salt, the change in free energy of moving a protein macro-ion of charge  $z_s$  will increase with increasing difference between the anion and cation self partition coefficients.

To predict  $K_s$  using Eq. (25), we must have an experimental method or model to determine each  $K_i^o$ . Here, we assume that within the approximations of Flory–Huggins theory, each  $K_i^o$  can be estimated by Eq. (19), provided the appropriate set of  $w_{ij}$  parameters describing all binary interactions are known. We also assume that the cation and anion of the added electrolyte are roughly of the same size and shape. This simplifies the resulting model significantly, as the entropic contributions to  $\ln K_A^o$  and  $\ln K_C^o$  cancel. Furthermore, if the dominant contributions to the self energy are the polymer–water interactions, which is a good approximation for dilute salt systems, the self energies of the top and bottom phases will cancel. Insertion of Eq. (19) into Eq. (25) then yields

$$\ln K_s = \ln K_s^o - \left( \frac{z_s}{z_+ - z_-} \right) \frac{M_{\text{ion}}}{RT} [(w_{tA} - w_{bA}) - (w_{tC} - w_{bC})] \quad (26)$$

where  $\ln K_s^o$  is given by Eq. (19) applied to the protein,  $M_{\text{ion}}$  is the size (degree of polymerization) of either ion, and  $w_{tA}$ , for instance, is the direct interaction energy of the anion for the top phase. What then does Eq. (26) tell us about the influence of added electrolyte on partitioning? To fix ideas, let us assume that the protein macro-ion carries a net positive charge  $z_s$  at the partitioning conditions (e.g., serum albumin). The quantity  $z_s/(z_+ - z_-)$  is then positive. Remembering that  $w$  becomes more negative when the direct interaction with a phase becomes more favorable, we see that Eq. (26) predicts that the protein will partition more strongly to the top phase if the anion (the counter-ion in this case) has a

more favorable direct interaction with the top phase than with the bottom, or if the cation (the co-ion) has a stronger affinity for the bottom phase. Moreover, Eq. (26) predicts that this effect will increase in direct proportion to the net positive charge  $z_s$  on the protein. All of these trends are observed experimentally.

Fig. 6 shows the data of Johansson and Hartman [12] describing the net-charge dependence and salt-type dependence of partitioning of serum albumin in the PEG 6000–dextran T-500 two-phase system at 2°C containing a single salt at an ionic strength of 100 mmol kg<sup>-1</sup>. When  $z_s = 0$ , Eq. (25) states that  $K_s = K_s^o$ . Thus, the self partition coefficient of serum albumin is ca. 0.35. The two salts used differ only in their anion (SO<sub>4</sub><sup>2-</sup> versus Cl<sup>-</sup>), which serves as the co-ion to albumin. Since K<sup>+</sup> is the cation in both cases,  $w_{tC} - w_{bC}$  is essentially the same in the two systems and can be treated as constant. Thus, differences in the effect of the added electrolyte can be solely attributed to the tendency of the anion to self-partition unevenly. According to Eq. (26),  $K_s$  will increase relative to  $K_s^o$  when an anion which interacts more favorably with the dextran-rich phase is chosen. This makes exchange of anions in the PEG-rich phase with protein macro-ions an energetically favorable process. We see that the SO<sub>4</sub><sup>2-</sup> ion

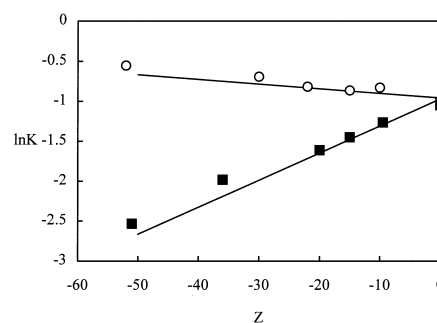


Fig. 6. Partitioning of differently charged serum albumin in PEG6000–dextran T500 two phase system.  $z$  is albumin charge. System composition: 4% PEG, 5% dextran, 0.1 mol/kg KCl or 0.05 mol/kg K<sub>2</sub>SO<sub>4</sub>. Protein concentration: 0.01%. Experimental data from [12]. KCl (■), K<sub>2</sub>SO<sub>4</sub> (○). The solid lines represent calculated partitioning. Interaction parameters (J/mol):  $w_{iK} = 0$ , for  $i = 1, 2, 3$  and  $a$ ,  $w_{KC} = -20\,000$ .  $w_{tC} = -5000$ ,  $w_{tS} = -3500$ ,  $w_{bC} = -1000$  and  $w_{bS} = -1000$ .  $w_{tA} = -5000$ ,  $w_{tS} = -200$ ,  $w_{bA} = -1000$  and  $w_{bS} = -1000$ . Subscripts K, C, S and  $a$  are K<sup>+</sup>, Cl<sup>-</sup>, SO<sub>4</sub><sup>2-</sup> and albumin, respectively. All other parameters are listed in Table 1.

increases the  $K_s$  of the negatively charged protein, indicating that the direct interaction of the ion with the dextran-rich phase is more favorable and thus,  $w_{tA} - w_{bA}$  is positive. The chloride ion causes a decrease in  $K_s$ , consistent with a more favorable direct interaction of  $\text{Cl}^-$  with the PEG-rich phase. The dielectric constant (and polarity) of the PEG-rich phase is lower than that of the bottom phase. Thus, an ion's relative attraction for the dextran-rich phase should scale with  $q_i^2/r$ , where  $q_i$  is the charge of ion  $i$  and  $r$  is the ionic radius [ $(q_i^2/r)_{\text{SO}_4^{2-}} > (q_i^2/r)_{\text{Cl}^-}$ ].

Eq. (26) predicts that the same salt effect on the partitioning of serum albumin can be achieved by changing the cation (counter-ion) of the salt. In this case however,  $K_s$  is predicted to increase relative to  $K_s^o$  when the ion interacts more favorably with the PEG-rich phase. This then increases the energetic reward for transferring the neutral complex (protein + counter-ions) to the PEG-rich phase.

Towards the goal of selecting the most appropriate phase system for a given separation, Eq. (26) tells us that in order to obtain extreme partitioning in PEG–dextran systems, the chosen salt should be composed of anions and cations with large and opposite direct interaction energies. For instance, the anion and cation should have very different surface-charge densities and/or hydrophilicities.

## 6. Conclusions

The complex properties and variety of aqueous two-phase partition systems have driven the need for a fundamental, yet simple model which practitioners of two-phase technology can use to better understand their systems and industries can use for process design and optimization. We show here that Flory–Huggins theory, when properly formulated, provides a number of simple analytical expressions which identify and quantify the fundamental driving forces governing phase behavior, protein partitioning, and salt effects in aqueous two-phase systems. The enthalpic driving force for protein partitioning is composed of two terms: one which describes the direct interaction between the protein (solute) and an average phase lattice site, and another which quantifies the enthalpy (termed the phase self-energy)

required to form a phase from the pure (solute-free) components. The more negative the direct-interaction term, the greater the tendency for the protein to partition to that phase. The protein will also have a preference for the phase with the higher (more positive) self energy.

Entropy can also drive uneven partitioning. In the absence of enthalpic effects, a protein will partition to the phase with the highest number of molecules per volume unit. Finally, the partitioning of a charged protein  $s$ , in a system containing a single electrolyte, can be calculated without knowledge of an interfacial electrostatic potential difference  $\Delta\psi$ . To predict  $K_s$ , one must only determine the self-partition coefficient  $K_i^o$  of each charged component, which we assume can be calculated (as least qualitatively) using Flory–Huggins theory.

It is important to note that Eqs. (7), (12), (23), (25) are exact. Any errors that result from our calculations are therefore due to the limitations of the Flory–Huggins theory. Given the fact that the Flory–Huggins theory does not, for instance, explicitly account for charge effects (although appropriate setting of the  $w_{ij}$  parameters deals with this problem to some extent), we expect the results to be qualitatively correct but not necessarily quantitatively correct. Nevertheless, the model appears to capture all of the general trends and fundamental properties of aqueous two-phase systems. If one requires precise quantitative information for a particular system, the application of a more detailed statistical–mechanical model such as the integral-equation theory of Haynes et al. [18] to the calculation of  $K_i^o$  or phase compositions may be warranted. However, compared to the Flory–Huggins theory approach described here, none of these models provides as clear a physical picture of the fascinating nature of phase behavior and partitioning in aqueous two-phase systems.

## References

- [1] P.Å. Albertsson, *Nature* 177 (1956) 771.
- [2] P.Å. Albertsson, *Partition of Cell Particles and Macromolecules*, 3rd ed., Wiley, New York, 1986.
- [3] S. Saeki, N. Kuwahara, M. Nakata, M. Kaneko, *Polymer* 17 (1976) 685.

- [4] I.Y. Galaev, B. Mattiasson, *Enzyme Microb. Technol.* 15 (1993) 354.
- [5] H.-O. Johansson, G. Karlström, F. Tjerneld, *Macromolecules* 26 (1993) 4478.
- [6] H.-O. Johansson, G. Karlström, B. Mattiasson, F. Tjerneld, *Bioseparation* 5 (1995) 269–279.
- [7] H.-O. Johansson, G. Karlström, F. Tjerneld, *Biochim. Biophys. Acta* 1335 (1997) 315–325.
- [8] P.A. Alred, A. Kozłowski, J.M. Harris, F. Tjerneld, *J. Chromatogr. A* 659 (1994) 289.
- [9] K. Berggren, H.-O. Johansson, F. Tjerneld, *J. Chromatogr. A* 718 (1995) 67.
- [10] H.-O. Johansson, G. Lundh, G. Karlström, F. Tjerneld, *Biochim. Biophys. Acta* 1290 (1996) 289–298.
- [11] G. Johansson, *Acta Chem. Scand. Ser. B* 28 (1974) 873.
- [12] G. Johansson, A. Hartman, *Proc. Int. Solvent Ext. Conf. Lyon, Soc. Chem. Ind.* 1 (1974) 927–942.
- [13] C.A. Haynes, J. Carson, H.W. Blanch, J.M. Prausnitz, *AIChE J.* 37 (1991) 1401.
- [14] A. Pfennig, A. Schwerin, *Fluid Phase Equilibria* 108 (1995) 305.
- [15] M. Svensson, F. Joabsson, P. Linse, F. Tjerneld, *J. Chromatogr. A* 761 (1997) 91–101.
- [16] C. Liu, D.T. Kamei, D.I.C. Wang, D. Blankschtein, *Bio-separations Using Two-Phase Aqueous Micellar Systems-An Overview*, presented at the 10th International Conference on Partitioning in Aqueous Two-Phase Systems, Reading, UK, August, 1997.
- [17] D.E. Brooks, K.A. Sharp, D. Fisher, *Theoretical Aspects of Partitioning in*: H. Walter, D.E. Brooks, D. Fisher (Editors), *Partitioning in Aqueous Two-Phase Systems*. Academic Press, Orlando, FL, 1985.
- [18] C.A. Haynes, F.J. Benitez, H.W. Blanch, J.M. Prausnitz, *AIChE J.* 39 (1993) 1539.
- [19] M. Kabiri-Badr, H. Cabezas, *Fluid Phase Equilibria* 115 (1996) 39–58.
- [20] F. Döbert, A. Pfennig, M. Stumpf, *Macromolecules* 28 (1995) 7860–7868.
- [21] H. Cabezas, *J. Chromatogr. B* 680 (1996) 3–30.
- [22] P.J. Flory, *J. Chem. Phys.* 10 (1942) 51.
- [23] M.L. Huggins, *J. Chem. Phys.* 46 (1942) 151.
- [24] E.A. Guggenheim, *Proc. R. Soc. London A* 183 (1944) 203.
- [25] A.M. Nemirovsky, M.G. Bawendi, K.F. Freed, *J. Chem. Phys.* 87 (1987) 7272.
- [26] P.J. Flory, *Principles of Polymer Chemistry*, Cornell Press, New York, 1953.
- [27] C.A. Haynes, Ph. D. Thesis, *Separation of Protein Mixtures by Extraction: Statistical–Mechanical Models of Aqueous Solutions Containing Polymers, Salts, and Globular Proteins*, University of California, Berkeley, CA, 1992.
- [28] C.A. Haynes, R.A. Beynon, R.S. King, H.W. Blanch, J.M. Prausnitz, *J. Phys. Chem.* 93 (1989) 5612.
- [29] H. Tompa, *Polymer Solutions*, Butterworths, London, 1956.
- [30] S.J. Rathbone, C.A. Haynes, H.W. Blanch, J.M. Prausnitz, *Macromolecules* 23 (1990) 3944–3947.
- [31] C.C. Hsu, J.M. Prausnitz, *Macromolecules* 7 (1974) 320–324.
- [32] R.S. King, H.W. Blanch, J.M. Prausnitz, *AIChE J.* 34 (1988) 1585.
- [33] A.D. Diamond, J.T. Hsu, *Biotech. Bioeng.* 34 (1989) 1000–1014.
- [34] M. Connemann, J. Gaube, U. Leffrang, S. Müller, A. Pfennig, *J. Chem. Eng. Data* 36 (1991) 446–448.
- [35] P.Å. Albertsson, A. Cajjarville, D.E. Brooks, F. Tjerneld, *Biochim. Biophys. Acta* 926 (1987) 87–93.
- [36] D. Forciniti, C.K. Hall, M.R. Kula, *Biotech. Bioeng.* 38 (1991) 986–994.
- [37] E.A. Guggenheim, *Thermodynamics*, 5th ed., North-Holland Publishing, 1967.
- [38] P.Å. Albertsson, *Partition of Cell Particles and Macromolecules*, 4th ed., Wiley, New York, 1997.